Isomers of OCS 2 : IR absorption spectra of OSCS and O(CS 2) in solid Ar

Wen-Jui Lo, Hui-Fen Chen, Po-Han Chou, and Yuan-Pern Lee

Citation: The Journal of Chemical Physics **121**, 12371 (2004); doi: 10.1063/1.1822919
View online: http://dx.doi.org/10.1063/1.1822919
View Table of Contents: http://scitation.aip.org/content/aip/journal/jcp/121/24?ver=pdfcov
Published by the AIP Publishing

Isomers of OCS_2: IR absorption spectra of OSCS and $O(CS_2)$ in solid Ar

Wen-Jui Lo[a)]
Department of Nursing, Tzu Chi College of Technology, 880, Sec. 2, Chien Kuo Road, Hualien 970, Taiwan

Hui-Fen Chen and Po-Han Chou
Department of Chemistry, National Tsing Hua University, 101, Sec. 2, Kuang Fu Road, Hsinchu 30013, Taiwan

Yuan-Pern Lee[b)]
Department of Applied Chemistry and Institute of Molecular Sciences, National Chiao Tung University, 1001, Ta-Hsueh Road, Hsinchu 30010, Taiwan, and Institute of Atomic and Molecular Sciences, Academia Sinica, Taipei 106, Taiwan

(Received 17 August 2004; accepted 30 September 2004)

Irradiation of an Ar matrix sample containing O_3 and CS_2 with a KrF excimer laser at 248 nm yielded new lines at 1402.1 (1404.7), 1056.2 (1052.7), and 622.3 (620.5) cm^{-1}; numbers in parentheses correspond to species in a minor matrix site. Secondary photolysis at 308 nm diminished these lines and produced mainly OCS and SO_2. Annealing of this matrix to 30 K yielded a second set of new lines at 1824.7 and 617.8 cm^{-1}. The first set of lines are assigned to C═S stretching, O–S stretching, and S–C stretching modes of carbon disulfide S-oxide, OSCS; and the second set of lines are assigned to C═O stretching and OCS bending modes of dithiiranone, $O(CS_2)$, respectively, based on results of ^{34}S- and ^{18}O-isotopic experiments and quantum-chemical calculations. These calculations using density-functional theory (B3LYP/aug-cc-pVTZ) predict four stable isomers of OCS_2: $O(CS_2)$, SSCO, OSCS, and SOCS, listed in order of increasing energy. According to calculations, $O(CS_2)$ has a cyclic CS_2 moiety and is the most stable isomer of OCS_2. OSCS is planar, with bond angles $\angle OSC \cong 111.9°$ and $\angle SCS \cong 177.3°$; it is less stable than SSCO and $O(CS_2)$ by ~102 and 154 kJ mol^{-1}, respectively, and more stable than SOCS by ~26 kJ mol^{-1}. Calculated vibrational wave numbers, IR intensities, ^{34}S- and ^{18}O-isotopic shifts for OSCS and $O(CS_2)$ fit satisfactorily with experimental results. © *2004 American Institute of Physics.*
[DOI: 10.1063/1.1822919]

I. INTRODUCTION

The reaction of O atom with CS_2 is important in the atmosphere, especially for the sulfur cycle.[1,2] Three product channels have been reported:

$$O(^3P) + CS_2 \rightarrow CS + SO, \quad \Delta H^\circ = -81 \text{ kJ mol}^{-1} \quad (1a)$$

$$\rightarrow OCS + S, \quad \Delta H^\circ = -228 \text{ kJ mol}^{-1} \quad (1b)$$

$$\rightarrow CO + S_2, \quad \Delta H^\circ = -348 \text{ kJ mol}^{-1}, \quad (1c)$$

with a total rate coefficient of $\sim 3.6 \times 10^{-12}$ cm^3 $molecule^{-1}$ s^{-1};[3] the enthalpy changes of these reactions are derived from JANAF thermochemical tables.[4] Reaction (1a) is the major channel; it proceeds via direct abstraction to form two reactive species CS and SO.[5,6] Reaction (1b) is responsible for converting CS_2 into OCS in the atmosphere, and for production of S atoms in combustion processes.[2] The reported branching ratio of reaction (1b) varies from 0.015 to 0.30,[7–9] but a more recent investigation supports a value ~0.09.[10] The branching ratio of reaction (1c) is reported to range from 0.03 to 0.20.[9–11] All reactions (1a)–(1c) are important in modeling the CO chemical laser system that utilizes the reaction,[12]

$$O(^3P) + CS \rightarrow CO^* + S(^3P), \quad \Delta H^\circ = -363 \text{ kJ mol}^{-1}. \quad (2)$$

In such a system, all three channels of reaction (1) are important: Reaction (1c) produces vibrationally excited CO, reaction (1b) produces OCS that enhances the population inversion of CO because OCS efficiently quenches CO in its lower vibrationally excited states, and reaction (1a) produces CS that directly participates in reaction (2). The small branching ratios of reactions (1b) and (1c) indicate that barriers for these reactions might be large and that the adduct OCS_2 plays an important role. Similarly, OCS_2 might also play an important role in the reaction

$$S(^3P) + OCS \rightarrow CO + S_2, \quad \Delta H^\circ = -121 \text{ kJ mol}^{-1}, \quad (3)$$

which is important in combustion systems.

Froese and Goddard performed quantum-chemical calculations on reaction (1) and located five stable isomers of OCS_2.[13] Jones and Taube[14] photolyzed Ar and Xe matrices containing O_3 and CS_2 with several conventional light sources and observed products OCS, SO_2, and SO_3, with

a)Author to whom correspondence should be addressed. Electronic mail: wjl@tccn.edu.tw
b)Author to whom correspondence should be addressed. Electronic mail: yplee@mail.nctu.edu.tw

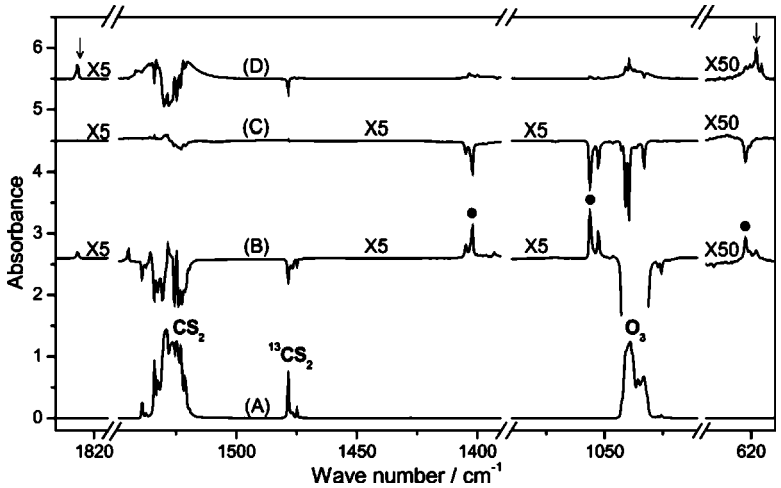

FIG. 1. Partial IR absorption spectrum of an $O_3/CS_2/Ar$ (2/1/600) matrix sample before irradiation (a), difference spectrum after irradiation at 248 nm for 15 min (b), difference spectrum after further irradiation of the matrix at 308 nm for 1 min (c), and difference spectrum after annealing of the matrix sample at 30 K for 10 min (d). New lines of group *A* and *B* are marked as ● and ↓ in traces (b) and (d), respectively.

CO being produced in minor proportion. These authors suggested that the primary channels for $O(^1D)+CS_2$ are production of $OCS+S$ and $CO+S_2$, and that with OCS as substrate the primary products are CO_2+S and $CO+SO$; no evidence was found for species OCS_2.

Utilizing selective photodissociation with a laser to avoid secondary photolysis on species of interest,[15–17] we produced numerous sulfur compounds that are difficult to form either in the gaseous phase or with a conventional light source.[18–26] Here we report a theoretical investigation of possible isomers of OCS_2 and the experimental production and infrared identification of OSCS and $O(CS_2)$ by irradiation of Ar matrix samples containing O_3 and CS_2 with laser emission at 248 nm and 308 nm.

II. EXPERIMENTS

The experimental setup is similar to that described previously.[18,23] A copper plate coated with platinum and cooled to ~13 K serves as a substrate for a cold matrix sample and as a mirror to reflect incident infrared (IR) beam to the detector. Typically gaseous mixtures of 6 mmol of O_3/Ar (1/200) and 3 mmol of CS_2/Ar (1/200) were codeposited over a period of 2 h. A KrF excimer laser (248 nm, operated at 10 Hz with energy ~4 mJ pulse^{-1}) was employed to photodissociate O_3. A XeCl excimer laser (308 nm, operated at 10 Hz with energies ~4 mJ pulse^{-1}) was used for secondary photolysis. IR absorption spectra were recorded with an evacuable Fourier-transform infrared (FTIR) spectrometer (Bomem, DA8) equipped with a KBr beam splitter and a Hg/Cd/Te detector (cooled to 77 K) to cover the spectral range 500–4000 cm^{-1}. Typically 600 scans with resolution of 0.5 cm^{-1} were recorded at each stage of the experiment.

O_2 (99.99%, Scott Specialty Gases), $^{18}O_2$ (MSD Isotopes, isotopic purity >96.5%), and Ar (99.999%, Scott Specialty Gases) were used without further purification. CS_2 (99.9%, Tedia) and $^{34}SC^{34}S$ (Cambridge Isotope Laboratories, listed isotopic purity of 90%) were degassed at 77 K. Scrambled ^{32}S- and ^{34}S-isotopic species were produced by mixing $^{32}SC\,^{32}S$ and $^{34}SC\,^{34}S$ in equal proportions in a Pyrex vacuum manifold followed by electric discharge with a Tesla coil for a few minutes. O_3 was produced and collected at 77 K after electric discharge of a small amount of O_2 with a Tesla coil.

III. COMPUTATIONAL METHOD

The equilibrium structure, vibrational frequencies, IR intensities, and energies were calculated with the GAUSSIAN03 program.[27] We used density-functional theory (DFT) for calculations; the B3LYP method uses Becke's three-parameter hybrid exchange functional,[28] and a correlation functional of Lee, Yang, and Parr,[29,30] with both local and nonlocal terms. Dunning's correlation-consistent polarized valence triplet-ζ basis set, augmented with *s*, *p*, *d*, and *f* functions (aug-cc-pVTZ), was used in all methods. Analytic first derivatives were utilized in geometry optimization and vibrational frequencies were calculated analytically at each stationary point.

IV. RESULTS AND DISCUSSION

A. Experimental observations and assignments

1. Experiments with O_3 and CS_2 in natural abundance

The IR spectrum of a sample of $O_3/CS_2/Ar$ (2/1/600) at 13 K exhibits multiple lines due to O_3 (1039.2 and 703.6 cm^{-1}) (Ref. 31) and CS_2 (2825.5, 2323.6, 2178.0, and 1528.8 cm^{-1}).[20,32] Lines at 2248.6, 2127.8, and 1478.4 cm^{-1} are due to $^{13}CS_2$,[20] whereas lines at 2803.7, 2318.1, 2165.2, and 1525.2 cm^{-1} are due to $^{32}SC\,^{34}S$.[32] A partial spectrum of the matrix sample before and after photolysis is shown in traces(a) and (b) of Fig. 1, respectively; trace(b) is a difference spectrum after irradiation of the matrix sample at 248 nm for 15 min. The difference spectrum was derived on subtracting the spectrum recorded in the preceding stage of irradiation/annealing from a new spectrum; a positive feature indicates production, whereas a negative feature indicates destruction.

After irradiation, lines at 2048.7, 858.8, and 522.5 cm^{-1} are readily assigned to OCS, lines at 1351.8, 1150.3, and 519.0 cm^{-1} are assigned to SO_2,[19,33] and a line at 1270.9 cm^{-1} is readily assigned to CS;[34,35] weak lines due to SO_3 (1384.3, 528.9, 489.7 cm^{-1}), S_2O (1157.6, 673.7 cm^{-1}),[24,36]

TABLE I. Wave numbers (in cm^{-1}) of lines observed for $O_3/CS_2/Ar$ matrix samples after irradiation at 248 nm.

Group *A*	C═S stretch (ν_1)	O–S stretch (ν_2)	S–C stretch (ν_3)
$^{16}O\,^{32}SC\,^{32}S$	1402.1 (1404.7)	1056.2 (1052.7)	622.4 (620.5)
$^{16}O\,^{34}SC\,^{32}S$	1400.7 (1402.8)	1045.9[a]	615.1
$^{16}O\,^{32}SC\,^{34}S$	1396.4 (1398.6)	1056.2 (1052.7)	618.1
$^{16}O\,^{34}SC\,^{34}S$	1394.9 (1397.0)	1045.9[a]	610.7
$^{18}O\,^{32}SC\,^{32}S$	1401.7 (1403.9)	1018.0 (1015.1)	620.0
Group *B*	C═O stretch (ν_1)		OCS bend (ν_3)
$^{16}O(C\,^{32}S_2)$	1824.7		617.8
$^{16}O(C\,^{32}S\,^{34}S)$	1824.7		617.5[b]
$^{16}O(C\,^{34}S_2)$	1824.7		617.0[b]
$^{18}O(C\,^{32}S_2)$	1787.4		613.8

[a]Lines associated with the minor site are overlapped with lines of O_3.
[b]Deconvolution of overlapped lines.

and SO (1138.5 cm^{-1}) (Ref. 37) are also identified. New lines at 1404.7, 1402.1, 1056.2, 1052.7, 622.3, 620.5 cm^{-1} [group *A*, marked ● in Fig. 1(b)] diminished slightly after the temperature of the matrix was raised to ~30 K for 10 min. Because relative intensities of the doublets at (1402.1, 1404.7), (1056.2, 1052.7), and (622.3, 620.5) cm^{-1} vary with deposition conditions and annealing, they are likely due to site splitting; wave numbers listed first in each pair are associated with the major site. Further irradiation of the matrix sample with laser emission at 308 nm for 1 min diminished these new lines nearly completely, as illustrated in the difference spectrum shown in trace(c) of Fig. 1; OCS appeared as a major product and SO_2 as a minor product (not shown). After annealing of the irradiated matrix to 30 K, new lines at 1824.7 and 617.8 cm^{-1} [group *B*, marked ↓ in trace(d) of Fig. 1] enhanced; these lines were present but with small intensities upon irradiation at 248 nm and diminished after further irradiation at 308 nm. Wave numbers of these new lines are listed in Table I.

We also employed alternative matrix hosts to explore the possibility of eliminating multiple matrix site splitting of group *A* but were unsuccessful. Multiplet structures (in decreasing order of intensity) were observed at (1402.6, 1404.5, 1406.6, 1410.7), (1049.6, 1046.6, 1047.9), and 624.0 cm^{-1} for a N_2 matrix host, and at (1396.1,1398.3), (1051.5, 1047.8), and 619.9 cm^{-1} for a Kr matrix host; these observations also support the assignment of multiple lines to site splitting. Hence all isotopic experiments were performed with Ar as a matrix host.

2. Isotopic experiments and assignments of group A

^{34}S-isotopic experiments. An isotopic mixture containing $^{32}SC\,^{32}S$, $^{32}SC\,^{34}S$, and $^{34}SC\,^{34}S$ in approximate proportions 1.00:1.10:1.07 was used in one experiment. An expanded difference spectrum of the ^{32}S-, ^{34}S-mixed $O_3/CS_2/Ar$ (2/1/600) matrix sample in regions 606–626, 1005–1025, 1044–1062, and 1381–1417 cm^{-1} after laser irradiation at 248 nm is shown in trace(b) of Fig. 2. Trace(a) of Fig. 2 depicts the corresponding difference spectrum of an $O_3/CS_2/Ar$ (2/1/600) matrix sample in natural abundance. Line positions of ^{34}S-substituted species are listed in Table I.

The doublet at 1402.1 and 1404.7 cm^{-1} splits into six lines. After deconvolution, we located four doublets having similar intensity ratios, shown as stick lines in trace(b) of Fig. 2; a detailed deconvolution plot is also shown below the trace. The wave numbers for the three additional doublets are (1400.7, 1402.8), (1396.4, 1398.6), and (1394.9, 1397.0) cm^{-1}. The ^{34}S-isotopic pattern indicates that two nonequivalent S atoms are involved in this mode. The ^{34}S-isotopic ratio 1394.9/1402.1=0.9949, defined as a ratio of vibrational wave number of the isotopically labeled species to that of the most naturally abundant species, is near to the theoretical values of 0.9919 for CS and 0.9954 for $CS_2(\nu_3)$ than values of 0.9901 for SO or 0.9701 for S_2. It is likely that this mode is associated with a SCS moiety.

The doublet at 1056.2 and 1052.7 cm^{-1} splits into two doublets, but the one with the smaller wave number was overlapped by intense absorption of O_3; the only observed additional line lies at 1045.9 cm^{-1}. The ^{34}S-isotopic pattern indicates that mainly one S atom is involved in this mode.

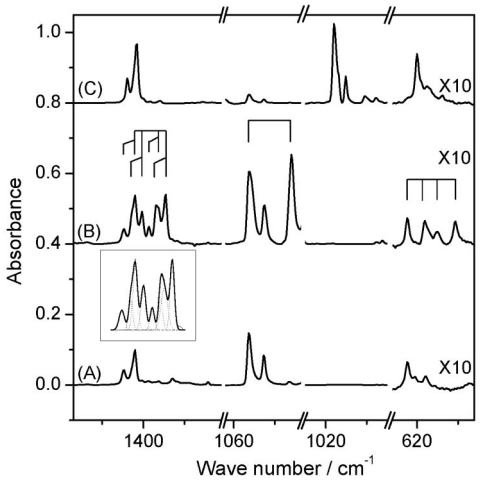

FIG. 2. Partial difference IR absorption spectra of lines in group *A* from $O_3/CS_2/Ar$ matrix samples with isotopic variants after irradiation at 248 nm for 15 min. (a) $O_3/CS_2/Ar$ (2/1/600), (b) $O_3/^{32}SC\,^{32}S/^{32}SC\,^{34}S/^{34}SC^{34}S/Ar$ (~6/1/1/1/1800); deconvolution of lines in the region 1390–1410 cm^{-1} is also shown below, and (c) $^{18}O_3/CS_2/Ar$ (2/1/600).

The ^{34}S-isotopic ratio of 1045.9/1056.2=0.9902 is near the theoretical value of 0.9901 for SO.

The line at 622.4 cm^{-1} split into four lines with additional lines at 618.1, 615.1, and 610.7 cm^{-1}; the ^{34}S-isotopic pattern indicates that two nonequivalent S atoms are involved in this mode. The ^{34}S-isotopic ratio of 610.7/622.4 =0.9812 is smaller than the theoretical value of 0.9919 for CS, but greater than a value of 0.9701 for S_2; this mode might involve mixed normal modes.

^{18}O-isotopic experiments. Experiments with $^{18}O_3$ were performed. An expanded difference spectrum of the $^{18}O_3/CS_2/Ar$ (2/1/600) matrix sample after laser irradiation at 248 nm is shown in trace(c) of Fig. 2; line positions of ^{18}O-substituted species are listed also in Table I. The doublet at 1402.1 and 1404.7 cm^{-1} shifts to 1401.7 and 1403.9 cm^{-1}. The ^{18}O-isotopic ratio 1401.7/1402.1=0.9997 is near unity, indicating that the O atom is only indirectly involved in this mode, consistent with the ^{34}S-isotopic pattern showing that this mode is likely associated with a SCS moiety. The doublet at 1056.2 and 1052.7 cm^{-1} shifts to 1018.0 and 1015.1 cm^{-1}. The ^{18}O-isotopic ratio of 1018.0/1056.2 =0.9638 is near the theoretical value of 0.9623 for SO. The line at 622.4 cm^{-1} shifts to 620.0 cm^{-1}. The ^{18}O-isotopic ratio of 620.0/622.4=0.9963 indicates that the O atom is involved only indirectly in this mode.

Assignments. Jones and Taube photolyzed a similar matrix with a medium-pressure Hg lamp, a low-pressure Hg lamp, and a Cd lamp, but they observed no evidence of absorption by OCS_2.[14] The most intense new band observed at 1402.1 cm^{-1} in this work overlapped with a broad feature that was assigned to SO_3 by Jones and Taube. In our previous work on photolysis of SO_3 we observed absorption of SO_3 at 2438.7, 1385.2, 527.1, and 490.3 cm^{-1}; hence the possibility that observed new lines are due to SO_3 is positively eliminated.[18,38]

Photodissociation of O_3 at 248 nm forms O and O_2. Reaction between CS_2 and O in a matrix is expected to produce various isomers of OCS_2, in addition to CS+SO, OCS+S, or CO+S_2 from the three channels observed in the gas phase. Because observed isotopic patterns indicate that the species contains a S–O bond and a SCS moiety with nonequivalent S atoms, and because the observed C–S stretching wave number (1402.1 cm^{-1}) is smaller than 1528 cm^{-1} of CS_2 (ν_3) but greater than 1271 cm^{-1} of CS, the new species is most likely OSCS rather than O(CS_2), SOCS, or SSCO. The nearly zero ^{18}O shift for the line at 1402.1 cm^{-1} and a small ^{18}O shift for the line at 622.3 cm^{-1} is consistent with a structure with the O atom bonding to an S atom of CS_2 so that the C═S bond (at 1402.1 cm^{-1}) remains nearly intact whereas the wave number of the C–S stretching mode (at 622.3 cm^{-1}) is slightly decreased upon ^{18}O substitution. Quantum chemical calculations provide further support for this assignment.

3. Isotopic experiments and assignments of group B

^{34}S-isotopic experiments. An expanded difference spectrum of lines in group *B* from the ^{32}S-, ^{34}S-mixed $O_3/CS_2/Ar$ (2/1/600) matrix sample, with $^{32}SC\,^{32}S$, $^{32}SC\,^{34}S$, and $^{34}SC\,^{34}S$ in approximate proportions 1.00:1.10:1.07, in regions 610–640 and 1780–1830 cm^{-1} after annealing of the matrix irradiated at 248 and 308 nm is shown in trace(b) of Fig. 3. Trace(a) of Fig. 3 depicts the corresponding difference spectrum of an $O_3/CS_2/Ar$ (2/1/600) matrix sample in natural abundance. Line positions of ^{34}S-substituted species are listed in Table I.

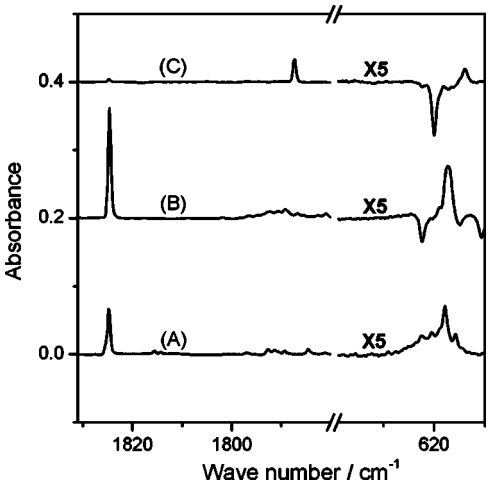

FIG. 3. Partial difference IR absorption spectra of lines in group *B* from $O_3/CS_2/Ar$ matrix samples with isotopic variants after irradiation at 248 nm for 15 min and at 308 nm for 1 min, followed by annealing at 30 K for 10 min. (a) $O_3/CS_2/Ar$ (2/1/600), (b) $O_3/^{32}SC\,^{32}S/^{32}SC\,^{34}S/^{34}SC^{34}S/Ar$ (~6/1/1/1/1800), and (c) $^{18}O_3/CS_2/Ar$ (2/1/600).

The line at 1824.7 cm^{-1} does not shift, indicating that S atom is not directly involved in this mode. The line at 617.8 cm^{-1} shifts to 617.5 cm^{-1} and its width increases from 0.85 to 1.99 cm^{-1}. This broad feature may be deconvoluted to three lines at 617.8, 617.5, and 617.0 cm^{-1} with ≈1:2:1 in intensity. The wave number and the ^{34}S-isotopic pattern indicate that S atom(s) is/are involved in this mode and this mode is likely associated with a nonstretching motion.

^{18}O-isotopic experiments. An expanded difference spectrum of lines in group *B* from the $^{18}O_3/CS_2/Ar$ (2/1/600) matrix sample after laser irradiation and annealing is shown in trace(c) of Fig. 3; line positions of ^{18}O-substituted species are listed also in Table I. The line at 1824.7 cm^{-1} shifts to 1787.4 cm^{-1}, indicating that the O atom is directly involved in this mode. The ^{18}O-isotopic ratio 1787.4/1824.7=0.9796 is near the theoretical value 0.9759 for CO. The line at 617.8 cm^{-1} shifts to 613.8 cm^{-1}; the ^{18}O-isotopic ratio of 613.8/617.8=0.9935 and the value of the wave number indicate that this mode is likely a bending mode involving the O atom.

Assignments. The ^{34}S-isotopic pattern provide insufficient information on how many S atoms are associated with this new species and we only know that the species contains a C–O bond and one or more S atoms. If we assume that this species is also an isomer of OCS_2, it is likely O(CS_2) rather than SSCO, SOCS, or OSCS because the observed C–O stretching wave number (1824.7 cm^{-1}) is much smaller than 2048.7 cm^{-1} of OCS and 2071.1 cm^{-1} of OCS^+ (Ref. 39), but greater than 1646.4 cm^{-1} of OCS^-.[39] The absence of ^{34}S shift for the line at 1824.7 cm^{-1} and a small ^{34}S shift for the line at 617.8 cm^{-1} are consistent with a structure with the O

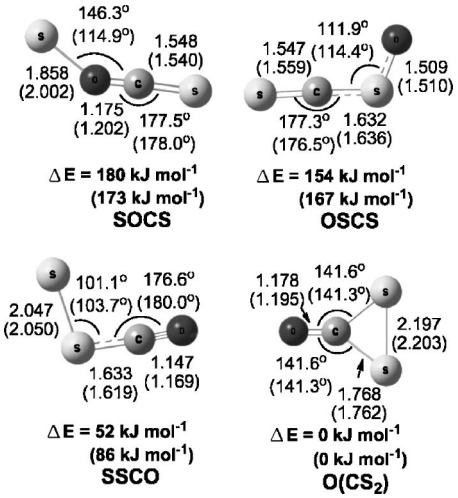

FIG. 4. Geometries and relative energies (in kJ mol^{-1}) of isomers of OCS_2 calculated with the B3LYP/aug-cc-pVTZ method. Relative energies are corrected with zero-point energies; the unit of bond length is in angstroms. Results from MP2/6-31G* are listed in parentheses.

atom bonding to a C atom of CS_2. Quantum chemical calculations provide further information on the assignment.

B. Comparison with calculations

We performed calculations using the B3LYP/aug-cc-pVTZ method to find four stable isomers of OCS_2: $O(CS_2)$, SSCO, OSCS, and SOCS, listed in order of increasing energy. Geometries and energies predicted for these species are shown in Fig. 4, with those predicted previously with second-order Møller–Plesset calculations (MP2/6-31G*) by Froese and Goddard listed parenthetically for comparison.[13] Froese and Goddard predicted also a fifth isomer oxathiiranethione S(COS) with a cyclic COS structure and a S atom doubly bonded to the cyclic moiety via the C atom, but we could locate no stable configuration for this species with B3LYP/aug-cc-pVTZ. The most stable isomer dithiiranone $O(CS_2)$ has a cyclic CS_2 structure and an O atom doubly bonded to the cyclic CS_2 moiety via the C atom. All three chain isomers have angular structures with a nearly linear triatomic moiety and we list the atom unassociated with the linear structure first. Isomers SOCS and SSCO, lying ~180 and 52 kJ mol^{-1} above $O(CS_2)$, have a nearly linear O–C–S moiety, whereas carbon disulfide S-oxide, OSCS, lying ~154 kJ mol^{-1} above $O(CS_2)$, has a nearly linear S–C–S moiety. The MP2/6-31G* method predicts structures similar to this work except for SOCS, for which the MP2 predicts a longer S–O bond (2.00 Å) and a smaller ∠SOC (114.9°) than those values (1.86 Å and 146.3°) predicted in this work with the B3LYP/aug-cc-pVTZ method. Both OSCS and SOCS are characterized by a short terminal C–S bond (~1.55 Å) similar to a double bond (cf. 1.54 Å for SCS and 1.56 Å for OCS);[40] the S–O bond length of OSCS (1.51 Å) is much smaller than that of SOCS (1.86 Å). In contrast, both SSCO and $O(CS_2)$ are characterized by a short C═O bond of length 1.15–1.18 Å.

Tables II and III list vibrational wave numbers, approximate mode description, and infrared intensities (in parentheses) of four isomers of OCS_2 predicted with B3LYP and MP2 methods. Observed vibrational wave numbers of lines of group *A* at 1402.1, 1056.2, and 622.3 cm^{-1} are near values (1437, 1031, 618 cm^{-1} from B3LYP and 1413, 1085, 597 cm^{-1} from MP2) predicted for ν_1 (C═S stretching), ν_2 (O–S stretching), and ν_3 (S–C stretching) modes of OSCS, respectively, but distinct from values predicted for other isomers of OCS_2; the ν_3 mode is mixed with some OSC bending motion. The observed ratio of integrated intensities for $\nu_1:\nu_2:\nu_3$, ~12:17:1, agrees satisfactorily with the ratio 17.6:16.5:1 for OSCS predicted with the B3LYP method.

Observed vibrational wave numbers of lines of group *B* at 1824.7 and 617.8 cm^{-1} are near values (1876, 610 cm^{-1} from B3LYP and 1783, 631 cm^{-1} from MP2) predicted for ν_1 (C═O stretching) and ν_3 (OCS bending) modes of $O(CS_2)$, respectively, but distinct from values predicted for other isomers of OCS_2. The observed ratio of integrated intensities for $\nu_1:\nu_3$, ~4.7:1, agrees satisfactorily with the

TABLE II. Vibrational wave numbers (in cm^{-1}) and infrared intensities of OSCS and $O(CS_2)$ predicted with two theoretical methods.

Species	Vibrational mode	Reference 13 MP2/6-31G*	This work B3LYP/aug-cc-pVTZ	This work /Ar matrix
OSCS	ν_1, C═S stretch	1413[a] (71)[b]	1436.6(194)[b]	1402.1, 1404.7
	ν_2, O–S stretch	1085 (168)	1031.1 (181)	1056.2, 1052.7
	ν_3, S–C stretch[c]	597(23.3)	617.6 (11)	622.3, 620.5
	ν_4, OSC bend[c]	456 (9.4)	483.0 (5)	
	ν_5, out-of-plane bend	238 (7.4)	283.1 (5)	
	ν_6, SCS bend	125 (3.5)	129.8 (4)	
$O(CS_2)$	ν_1, C═O stretch	1783 (427)	1876.2 (563)	1824.7
	ν_2, CS_2 sym. stretch	637(17.9)	660.6 (11)	
	ν_3, OCS bend	631 (148)	610.3 (114)	617.8
	ν_4, out-of-plane bend	486 (5.0)	521.1 (3)	
	ν_5, SCS bend	401 (0.2)	441.8 (0)	
	ν_6, CS_2 asymmetric bend	357 (5.4)	360.2 (6)	

[a]Scaled by 0.95, as listed in Ref. 13.
[b]IR intensities (in km mol^{-1}) are listed in parentheses.
[c]Mixed mode.

TABLE III. Vibrational wave numbers (in cm^{-1}) and infrared intensities of SOCS and SSCO predicted with two theoretical methods.

Species	Vibrational mode	This work B3LYP/aug-cc-pVTZ	Reference 13 MP2/6-31G*
SOCS	ν_1, C═S stretch	2021.0 (761)[a]	
	ν_2, C–O stretch	901.2 (17)	
	ν_3, OCS bend	490.2 (43)	
	ν_4, out-of-plane bend	439.6 (2)	
	ν_5, S–O stretch	296.5 (0)	
	ν_6, SOC bend	67.8 (9)	
SSCO	ν_1, C═O stretch	2089.0(824)	1963[b] (629)
	ν_2, S–C stretch	720.9 (4)	732 (11)
	ν_3, S–S bend[c]	494.9 (6)	456 (2)
	ν_4, SCO bend[c]	446.0 (10)	418 (12)
	ν_5, out-of-plane bend	402.6 (2)	367 (3)
	ν_6, SSC bend	110.7 (5)	83 (7)

[a]IR intensities (in km mol^{-1}) are listed in parentheses.
[b]Scaled by 0.95, as listed in Ref. 13.
[c]Mixed mode.

ratio 5:1 predicted for $O(CS_2)$ with the B3LYP method.

Table IV lists predicted ^{34}S- and ^{18}O-isotopic ratios of four isotopomers of OSCS and $O(CS_2)$. Predicted isotopic ratios for OSCS and $O(CS_2)$ are nearly the same as those determined experimentally (deviations <0.002, except for ν_3 of $O\,^{34}SCS$ and $O\,^{34}SC\,^{34}S$ that deviates up to 0.003). ^{34}S- and ^{18}O-isotopic ratios predicted for SOCS and SSCO are listed in Table V for comparison; they do not agree with our experimental results. Hence, based on observed ^{34}S- and ^{18}O-isotopic shifts and comparison with vibrational wave numbers and isotopic ratios predicted with theoretical calculations, we conclude that new absorption lines of group *A* at 1402.1 (1404.7), 1056.2 (1052.7), and 622.3 (620.5) cm^{-1} are associated with C═S stretching (ν_1), O–S stretching (ν_2), and S–C stretching (ν_3) vibrational modes of OSCS isolated in solid Ar, and new absorption lines of group *B* at 1824.7 and 617.8 cm^{-1} are associated with C═O stretching (ν_1) and OCS bending (ν_3) vibrational modes of $O(CS_2)$ isolated in solid Ar.

C. Mechanism of formation of OSCS

The absorption cross section of CS_2 at 248 nm is small, hence its photodissociation is relatively unimportant.[41] Photodissociation of O_3 at 248 nm forms $O(^1D)$ and O_2 with a quantum yield of 0.91 ± 0.06.[42,43] $O(^1D)$ might react with a nearest neighbor CS_2 to form CS+SO and other products before it relaxes to $O(^3P)$. After irradiation at 248 nm, pro-

TABLE IV. Experimental and calculated ^{34}S- and ^{18}O-isotopic ratios, defined as the ratio of vibrational wave numbers of a substituted isotopomer to that of the corresponding ^{32}S, ^{16}O species, of OSCS and $O(CS_2)$.

Species		ν_1	ν_2	ν_3	ν_4	ν_5	ν_6
$^{16}O\,^{34}SC\,^{32}S$	Calc.	0.9990	0.9904	0.9853	0.9953	0.9981	0.9970
	Expt.	0.9990 (0.9987)[a]	0.9902 (0.9903)[a]	0.9883			
$^{16}O\,^{32}SC\,^{34}S$	Calc.	0.9959	1.0000	0.9935	0.9920	0.9974	0.9948
	Expt.	0.9959 (0.9957)[a]	1.0000 (1.0000)[a]	0.9931			
$^{16}O\,^{34}SC\,^{34}S$	Calc.	0.9949	0.9904	0.9789	0.9871	0.9955	0.9919
	Expt.	0.9949 (0.9940)[a]	0.9902 (0.9903)[a]	0.9812			
$^{18}O\,^{32}SC\,^{32}S$	Calc.	1.0000	0.9621	0.9974	0.9907	1.0000	0.9715
	Expt.	0.9997 (0.9994)[a]	0.9638 (0.9643)[a]	0.9963			
$^{16}O(C\,^{32}S\,^{34}S)$	Calc.	1.0000	0.9929	0.9993	0.9995	0.9879	0.9902
	Expt.	1.0000		0.9995			
$^{16}O(C\,^{34}S_2)$	Calc.	1.0000	0.9857	0.9986	0.9991	0.9754	0.9806
	Expt.	1.0000		0.9987			
$^{18}O(C\,^{32}S_2)$	Calc.	0.9783	0.9809	0.9926	0.9902	0.9930	0.9808
	Expt.	0.9796		0.9935			

[a]Isotopic ratios for the species in a minor site are listed in parentheses.

TABLE V. Calculated ^{34}S- and ^{18}O-isotopic ratios, defined as the ratio of vibrational wave numbers of a substituted isotopomer to that of the corresponding ^{32}S, ^{16}O species, of SOCS and SSCO.

Species	ν_1	ν_2	ν_3	ν_4	ν_5	ν_6
$^{32}S\,^{16}OC\,^{32}S$	(2021.0)[a]	(901.2)	(490.2)	(439.6)	(296.5)	(67.8)
$^{32}S\,^{16}OC\,^{34}S$	0.9995	0.9877	0.9986	0.9982	0.9949	0.9959
$^{34}S\,^{16}OC\,^{32}S$	1.0000	0.9999	1.0000	1.0000	0.9822	0.9922
$^{34}S\,^{16}OC\,^{34}S$	0.9995	0.9877	0.9986	0.9982	0.9771	0.9879
$^{32}S\,^{18}OC\,^{32}S$	0.9847	0.9723	0.9880	0.9911	0.9909	0.9720
$^{32}S\,^{32}SC\,^{16}O$	(2089.0)[a]	(720.9)	(494.9)	(446.0)	(402.6)	(110.7)
$^{34}S\,^{32}SC\,^{16}O$	1.0000	0.9999	0.9902	0.9935	1.0000	0.9890
$^{32}S\,^{34}SC\,^{16}O$	0.9999	0.9863	0.9968	0.9882	0.9985	0.9935
$^{34}S\,^{34}SC\,^{16}O$	0.9999	0.9863	0.9877	0.9807	0.9985	0.9826
$^{32}S\,^{32}SC\,^{18}O$	0.9792	0.9797	0.9958	0.9948	0.9893	0.9792

[a]Calculated wave numbers for the ^{32}S-, ^{16}O-species are listed in parentheses.

duction of CS and SO is clearly indicated. That annealing of the matrix at 30 K decreases the intensity of OSCS slightly indicates that $O(^3P)$ might not react with CS_2. Theoretical calculations with the fourth-order Møller–Plesset (MP4SDTQ) method predict that formation of OSCS from $O(^3P)+CS_2(^1\Sigma_g^+)$ has a barrier of 77 kJ mol^{-1}, whereas that from $CS(^1\Sigma^+)+SO(^3\Sigma^-)$ has a barrier of 71 kJ mol^{-1};[13] both barriers are too large for the reactants at low temperature to overcome. Hence, formation of OSCS likely involves reaction of $O(^1D)$ with CS_2. Our observation of a decrease in intensity of OSCS upon annealing of the matrix at 30 K is consistent with the above mechanism; $O(^1D)$ relaxes to $O(^3P)$ shortly after irradiation at 248 nm.

When the $O_3/CS_2/Ar$ sample irradiated at 248 nm was irradiated further at 308 nm, lines due to OSCS disappeared, whereas lines due to OCS increased substantially and those due to SO_2 increased slightly; lines due to CS_2 remained unchanged. This observation indicates that at 308 nm OSCS likely photodissociates to form mainly OCS and S; S might further react with nearby O_2 to form SO_2. Further investigations of electronically excited states of OSCS and their photodissociation dynamics are needed.

Annealing of the above irradiated matrix enhanced lines due to $O(CS_2)$, indicating that the formation mechanism of $O(CS_2)$ is OCS+S rather than $O+CS_2$. According to calculations, the barrier for $O(^1D)+CS_2$ to form $O(CS_2)$ is ~90 kJ mol^{-1}.[13] The barrier for $S(^1D)+OCS$ to form $O(CS_2)$ is expected to be small. Quantum chemical calculations on the reaction of $S(^3P)+OCS$ to form $O(CS_2)$ was unreported, the intersystem crossing might lead to a path to form $O(CS_2)$ with a small barrier.

On the basis of spectral information of OSCS and $O(CS_2)$ obtained in this work, further experiments in the gaseous phase at low temperatures might be performed to investigate the adduct formation and equilibrium of reaction (1) so as to assess the importance of this reaction in atmospheric or combustion chemistry.

V. CONCLUSION

We irradiated matrix samples of $O_3/CS_2/Ar$ with a KrF excimer laser at 248 nm and observed new IR absorption lines at 1402.1 (1404.7), 1056.2 (1052.7), and 622.3 (620.5) cm^{-1}; wave numbers in parentheses are associated with a minor site. These new features are attributed to C═S stretching (ν_1), O–S stretching (ν_2), and S–C stretching (ν_3) modes of carbon disulfide S-oxide OSCS, respectively, based on observed ^{34}S- and ^{18}O-isotopic shifts and theoretical predictions of line positions, infrared intensities, and isotopic ratios for possible isomers of OCS_2. The product OSCS was likely formed mainly via reaction of $O(^1D)$ and CS_2 in the matrix; secondary photolysis at 308 nm depleted OSCS and produced mainly OCS. Annealing of the above irradiated matrix yielded new lines at 1824.7 and 617.8 cm^{-1} that may be attributed to dithiiranone $O(CS_2)$; these new features are attributed to C═O stretching (ν_1) and OCS bending (ν_3) modes, respectively. The product $O(CS_2)$ was likely formed mainly via reaction of S and OCS in the matrix. This work provides spectral information for future investigations of the atmospheric reaction of $O+CS_2$ or S+OCS at low temperatures using IR detection of OSCS or $O(CS_2)$.

ACKNOWLEDGMENTS

The authors thank the National Science Council of Taiwan (Grant No. NSC92-2113-M-007-033) and MOE Program for Promoting Academic Excellence of Universities (Grant No. 89-FA04-AA) for support and the National Center for High-Performance Computing for computer time. W.I.L. thanks the Institute of Atomic and Molecular Sciences, Academia Sinica for a short-term visiting professorship.

[1] B. M. R. Jones, R. A. Cox, and S. A. Penkett, J. Atmos. Chem. **1**, 65 (1983).
[2] V. V. Azatyan, Kinet. Catalysis **44**, 459 (2003).
[3] W. B. DeMore, S. P. Sander, D. M. Golden *et al.*, *Chemical Kinetics and Photochemical Data for Use in Stratospheric Modeling* (JPL publication 97-4, Pasadena, CA, 1997).
[4] M. W. Chase, Jr., J. Phys. Chem. Ref. Data Monograph **9** (1998).
[5] J. Geddes, P. N. Clough, and P. L. Moore, J. Chem. Phys. **61**, 2145 (1974).
[6] P. A. Gorry, C. V. Nowikow, and R. Grice, Mol. Phys. **37**, 329 (1979).
[7] G. Hancock and I. W. M. Smith, Trans. Faraday Soc. **67**, 2586 (1971).
[8] R. D. Suart, P. H. Dawson, and G. H. Kimbell, J. Appl. Phys. **43**, 1022 (1972).
[9] I. R. Slagle, J. R. Gilbert, and D. Gutman, J. Chem. Phys. **61**, 704 (1974).
[10] W. F. Cooper and J. F. Hershberger, J. Phys. Chem. **96**, 5405 (1992).
[11] D. S. Y. Hsu, W. M. Shaub, T. L. Burks, and M. C. Lin, Chem. Phys. **44**, 143 (1979).
[12] M. A. Pollack, Appl. Phys. Lett. **8**, 237 (1966).
[13] R. D. J. Froese and J. D. Goddard, J. Chem. Phys. **98**, 5566 (1993).
[14] P. R. Jones and H. Taube, J. Phys. Chem. **77**, 1007 (1973).

[15] B.-M. Cheng, J.-W. Lee, and Y.-P. Lee, J. Phys. Chem. **95**, 2814 (1991).
[16] W.-J. Lo and Y.-P. Lee, J. Chem. Phys. **101**, 5494 (1994).
[17] W.-J. Lo and Y.-P. Lee, Chem. Phys. Lett. **229**, 357 (1994).
[18] S.-H. Jou, M.-y. Shen, C.-h. Yu, and Y.-P. Lee, J. Chem. Phys. **104**, 5745 (1996).
[19] L.-S. Chen, C.-I. Lee, and Y.-P. Lee, J. Chem. Phys. **105**, 9454 (1996).
[20] M. Bahou, Y.-C. Lee, and Y.-P. Lee, J. Am. Chem. Soc. **122**, 661 (2000).
[21] M. Bahou, S.-F. Chen, and Y.-P. Lee, J. Phys. Chem. A **104**, 3613 (2000).
[22] W.-J. Lo and Y.-P. Lee, Chem. Phys. Lett. **336**, 71 (2001).
[23] M. Bahou and Y.-P. Lee, J. Chem. Phys. **115**, 10694 (2001).
[24] W.-J. Lo, Y.-J. Wu, and Y.-P. Lee, J. Chem. Phys. **117**, 6655 (2002).
[25] W.-J. Lo, Y.-J. Wu, and Y.-P. Lee, J. Phys. Chem. A **107**, 6944 (2003).
[26] W.-J. Lo, H.-F. Chen, Y.-J. Wu, and Y.-P. Lee, J. Chem. Phys. **120**, 5717 (2004).
[27] M. J. Frisch, G. W. Trucks, H. B. Schlegel *et al.*, GAUSSIAN03 Revision A.1 Gaussian Inc., Pittsburgh, PA, 2003.
[28] A. D. Becke, J. Chem. Phys. **98**, 5648 (1993).
[29] C. Lee, W. Yang, and R. G. Parr, Phys. Rev. B **37**, 785 (1988).
[30] B. Miehlich, A. Savin, H. Stoll, and H. Preuss, Chem. Phys. Lett. **157**, 200 (1989).
[31] P. Brosset, R. Dahoo, B. Gouthier-Roy, L. Abouaf-Marguin, and A. Lakhlifi, Chem. Phys. **172**, 315 (1993).
[32] A. Givan, A. Loewenschuss, K. D. Bier, and H. J. Jodl, Chem. Phys. **106**, 151 (1986).
[33] D. Maillard, M. Allavena, and J. P. Perchard, Spectrochim. Acta, Part A **31A**, 1523 (1975).
[34] R. B. Bohn, Y. Hannachi, and L. Andrews, J. Am. Chem. Soc. **114**, 6452 (1992).
[35] M. E. Jacox and D. E. Milligan, J. Mol. Spectrosc. **58**, 142 (1975).
[36] A. G. Hopkins, F. P. Daly, and C. W. Brown, J. Phys. Chem. **79**, 1849 (1975).
[37] A. G. Hopkins and C. W. Brown, J. Chem. Phys. **62**, 2511 (1975).
[38] V. E. Bondybey and J. H. English, J. Mol. Spectrosc. **109**, 221 (1985).
[39] C. L. Lugez, W. E. Thompson, and M. E. Jacox, J. Chem. Phys. **115**, 166 (2001).
[40] P. C. Cross and L. O. Brockway, J. Chem. Phys. **3**, 821 (1935).
[41] C. Y. R. Wu and D. L. Judge, Geophys. Res. Lett. **8**, 769 (1981).
[42] K. Takahashi, S. Hayashi, Y. Matsumi, N. Taniguchi, and S. Hayashida, J. Geophys. Res., [Atmos.] **107**, 4440 (2002).
[43] R. K. Talukdar, M. K. Gilles, F. BattinLeclerc, A. R. Ravishankara, J. M. Fracheboud, J. J. Orlando, and G. S. Tyndall, Geophys. Res. Lett. **24**, 1091 (1997).